Supporting Information

Improvement of Extraction Efficiency and Metabolites of Pollutants from Medium and Low Concentration Organic Polluted Soil

Xiaojuan Bai [1,2,*], Wei Song [2], Linlong Guo [2], Rujiao Liu [2], Yihan Cao [2], Pin Jin [2], Bowen Zhu [1,2] and Xiaoran Zhang [1,2]

[1] Centre for Urban Environmental Remediation, Beijing University of Civil Engineering and Architecture, Beijing 100044, China
[2] Beijing Energy Conservation & Sustainable Urban and Rural Development Provincial and Ministry Co-Construction Collaboration Innovation Center, Beijing University of Civil Engineering and Architecture, Beijing 100044, China
* Correspondence: baixiaojuan@bucea.edu.cn or heixia.1986@163.com

1. Extraction and Purification Method

1.1. Ultrasonication Extraction

The soil sample was accurately weighed using an analytical balance and thoroughly mixed with anhydrous sodium sulfate. The extraction solvent was added and placed in an ultrasonic cleaner for ultrasonic extraction. After sonication, the samples were centrifuged at 3000 rpm for 10 min using a high-speed centrifuge. This process was repeated three times to ensure complete extraction of the target contaminants. The supernatant obtained from each centrifugation was mixed and the volume was reduced to 1 mL using a rotary evaporator. extraction solvent was added to a final volume of 1.5 mL.

1.2. Soxhlet Extraction

The samples were dehydrated by vacuum freeze dryer, and the frozen samples were homogenized into fine particles of about 1 mm by sufficient grinding. Accurately weigh 20 g of contaminated soil sample, add 80.0 μL of alternative standard (mixture of acetone and hexane in a 1:1 ratio), carefully transfer all samples into filter paper, and place the filter paper in a Soxhlet extractor reflux tube. Add 100 mL of a mixture of acetone and hexane (1:1 ratio) to a round bottom solvent flask and control the reflux rate to 4–6 times per hour. Collect the extract solution.

1.3. Mechanical Shaking Extraction

The soil sample was placed in a glass container and the extraction solvent was added. The glass container was transferred to a multifunctional stirrer and the extraction was shaken at 180 revolutions per minute. After extraction, centrifuge at 3000 rpm for 10 min using a high speed centrifuge. This process was repeated three times to ensure complete extraction of the contaminants. The supernatant obtained from each centrifugation was mixed and concentrated using a rotary evaporator. Add the extraction solvent and adjust the volume to 1.5 mL.

1.4. Ultrasonic Cell Crusher Extraction

Mix the contaminated soil with the extraction solvent and perform the extraction using an ultrasonic cell disruptor with an input power of 1800 W and an ultrasonic frequency of 20.5 kHz. Optimize the extraction conditions by varying the ultrasonic switch-on time and the total extraction time.

1.5. Microwave Extraction

Thoroughly mix the soil sample with anhydrous sodium sulfate. Add the extraction solvent to the soil sample and place it in a microwave digestion vessel. Set the temperature and microwave time, and microwave

the sample. Allow the sample to cool to room temperature. Then, centrifuge the sample at a speed of 3000 rpm for 10 min. Repeat this process three times and combine the supernatant obtained from each centrifugation.

1.6. Purification and Concentration

Purification: The SPE column filled with Florisil was cleaned as follows: the Florisil column was activated with 5 mL of extractant, the concentrate was transferred to the Florisil column, the sample container was washed with 2 mL of extractant, and the effluent solvent was discarded; the measured target was adsorbed on the column, soaked with extractant, and eluted to receive the effluent water. The eluate was collected and concentrated using a rotary evaporator.

Concentration: The water bath temperature was set to 30–40°C, and the rotation speed was set to 100–120 rpm. The nitrogen blow concentration parameters were set as follows: the nitrogen gas flow rate was set to 1.8−2.2 L/min, and the glass tube was tilted at a certain angle to expose the maximum possible liquid surface area. The position of the nitrogen spray was periodically adjusted as the solvent evaporated.

Table S1. Ultrasonic and Mechanical Oscillation Extraction Parameter Settings.

Factors	Coded Levels		
Independent variables	−1	0	1
A: Liquid-to-solid ratio	1	2	3
B: Extraction time	10	15	20
C: Number of extractions	1	2	3
D: Extraction temperature	30	45	60

Table S2. Microwave extraction parameter Settings.

Factors	Coded Levels		
Independent variables	−1	0	1
A: Liquid-to-solid ratio	1	2	3
B: Extraction time	10	15	20
C: Number of extractions	1	2	3
D: Extraction temperature	50	60	70

2. DNA Extraction and Analysis of Microbial Community

Table S3. Instruments and Reagents.

Name	Manufacturer
2×Phanta Max Master Mix	Vazyme Biotech Co., Ltd.
QIA quick Gel Extraction Kit	Qiagen
AGENCOURT®AMPURE® XP Kit	Beckman Coulter, Inc.
KAPA Library Quantification Kit Illumina® Platforms	KAPA Biosystems
T100™ Thermal Cycler (PCR)	Bio-RAD Inc.
Qubit® Fluorometers (Fluorescence Quantification Instrument)	Thermo Fisher Scientific
Qseq100 DNA Analyzer	Bioptic Inc.
LightCycler® 96 (Real-time Quantitative PCR Instrument)	Roche Inc.

Table S4. Default primers and standard experimental conditions.

Amplification Primer Name	Primer Name	Primer Sequence (5′->3′)	Amplification Region	Target Fragment Length	Annealing Temperature
Bacterial 16S	B341F	CCTACGGGNGGCWGCAG	V3–V4	450	55
-	B785R	GACTACHVGGGTATCTAATCC	-	-	-

Experimental Steps

I. First Round of PCR Amplification

Table S5. Prepare the PCR reaction system.

Component	Volume of One Reaction
Metagenomic DNA (10–50 ng/μL)	X μL
2×Phanta Max Master Mix	12.5 μL
Specific Forward Primer（25 μM）	0.25 μL

Specific Reverse Primer（25 μM）	0.25 μL
PCR Grade Water	(12−X) μL
Total volume	25 μL

Table S6. Place the PCR tubes in the PCR machine and run the program.

CYCLE STEP	TEMP	TIME	CYCLES
Pre-denaturation	95 °C	3 min	1
Denaturation	95 °C	30 s	25
Annealing	-	30 s	
Extension	72 °C	30 s	
Final Extension	72 °C	5 min	1
Hold	4 °C	+∞	

Take 2 μL of the PCR product for 2% agarose gel electrophoresis to check the target fragment.

II. PCR Product Purification

Purify the PCR product using 1X volume of AMPure XP Beads.

III. Second Round of PCR Amplification

Table S7. Prepare the second round of the PCR reaction system.

Component	Volume of One Reaction
PCR product from the previous step	2.5 μL
2×Phanta Max Master Mix	12.5 μL
Specific Forward Primer（25 μM）	0.25 μL
Specific Reverse Primer（25 μM）	0.25 μL
PCR Grade Water	9.5 μL
Total volume	25 μL

Table S8. Place the PCR tubes in the PCR machine and run the program.

YCLE STEP	TEMP	TIME	CYCLES
Pre-denaturation	95 °C	3 min	1
Denaturation	95 °C	30 s	8
Annealing	Per reaction program	30 s	
Extension	72 °C	30 s	
Final Extension	72 °C	5 min	1
Hold	4 °C	+∞	

IV. Library Purification

Perform electrophoresis on a 2% agarose gel and then excise and recover the target fragments.
Conduct gel extraction using the QIAquick Gel Extraction Kit following the manufacturer's instructions.

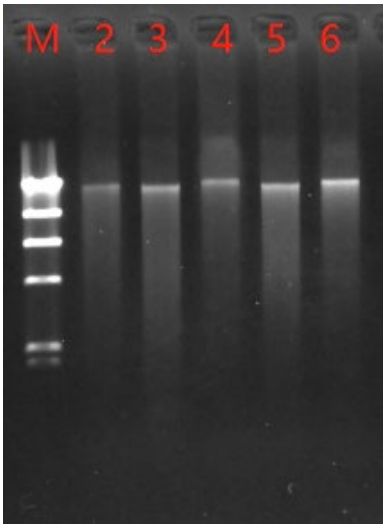

V. Library Quality Assessment and Quantification

Measure the library DNA's quality and concentration using a Qubit Fluorometer. A concentration greater than 1.0 ng/μL is considered acceptable.

Analyze the library DNA length distribution using a Qseq100 DNA Analyzer. It should exhibit the desired fragment length, a single peak, no adapter dimers, and no large fragment peaks to be considered acceptable.

Quantify the molar concentration of library DNA using the KAPA Library Quantification Kit as the standard for library pooling.

VI. Sequencing

After mixing and denaturing the library pools, load them onto the Illumina Novaseq 6000 sequencing platform for high-throughput parallel sequencing, using the PE250 sequencing mode.

3. Extraction Method Establishment

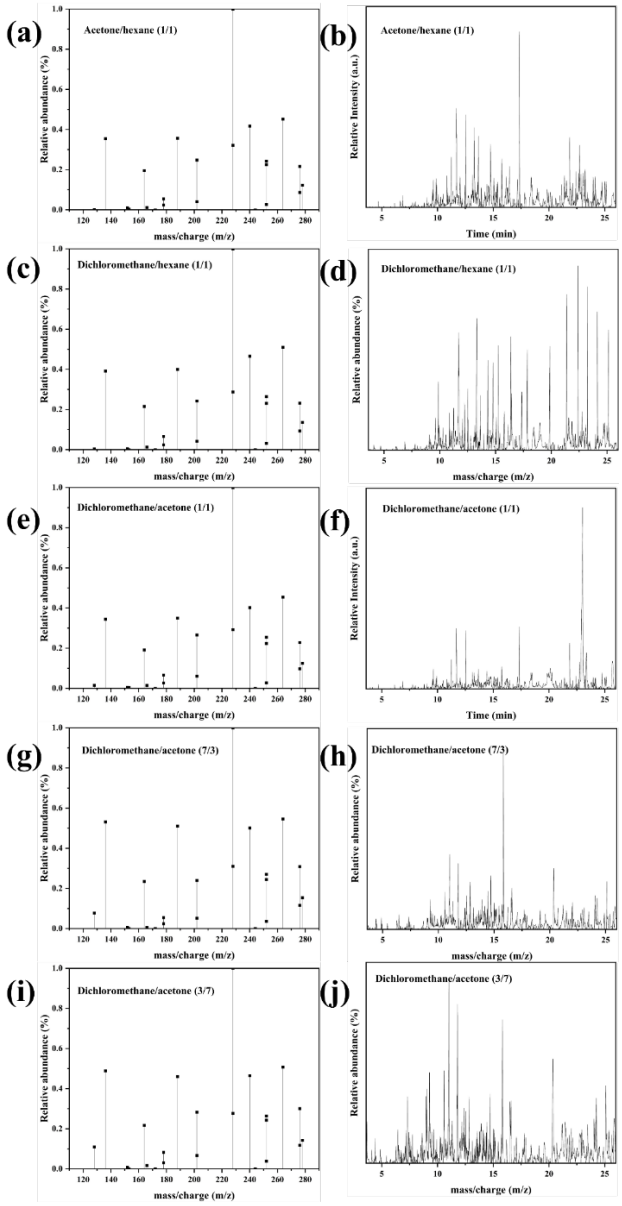

Figure S1. Optimized Chromatograms and Mass Spectra of Polycyclic Aromatic Hydrocarbons (PAH) Extractants.

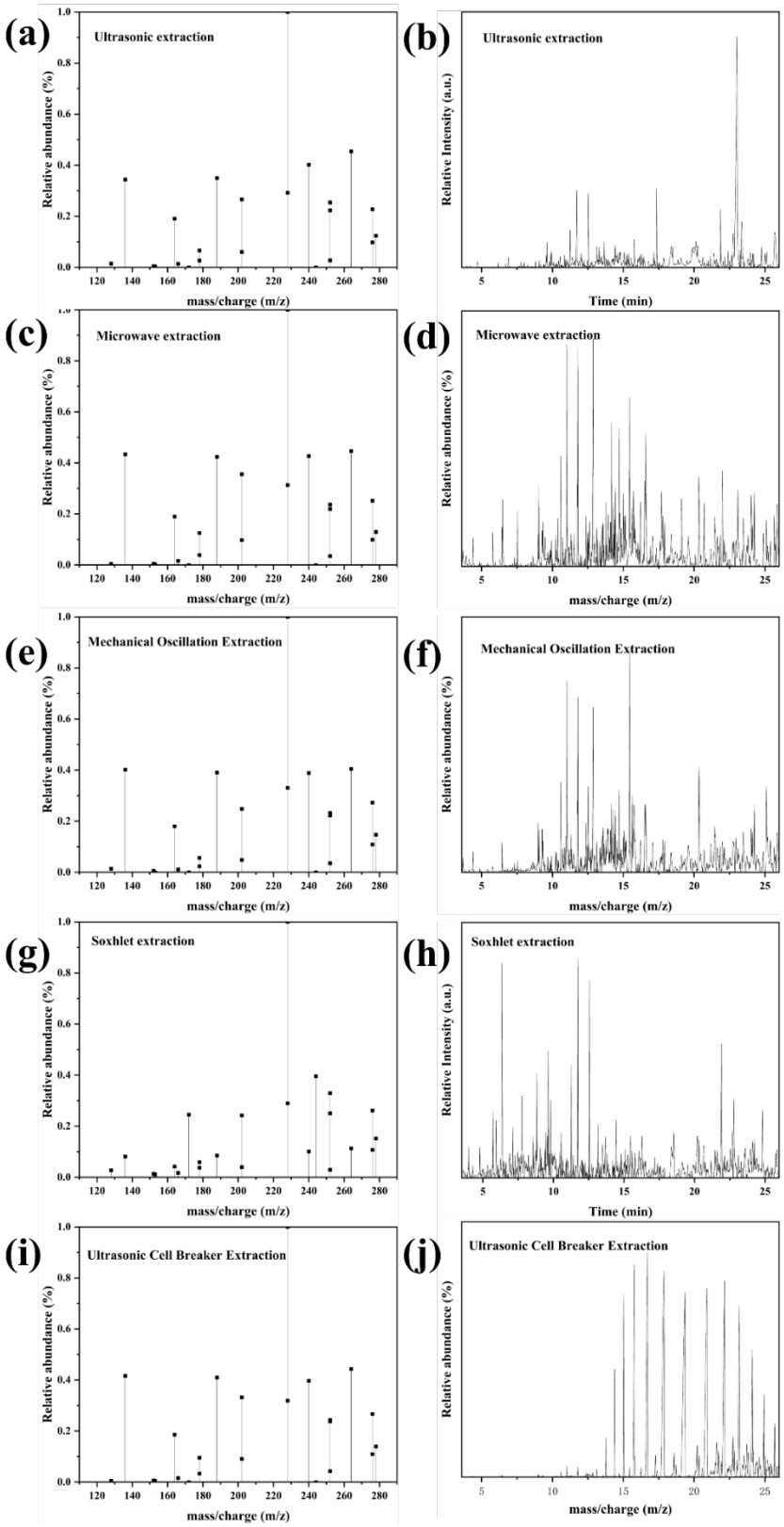

Figure S2. Optimization of extraction methods for polycyclic aromatic hydrocarbons by chromatography and mass spectrometry.

Table S9. Polycyclic aromatic hydrocarbon properties.

Name	Formula	*m/z* Ion (uma)	Abbreviation	Structure
Naphthalene	$C_{10}H_8$	128	NAP	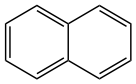
Acenaphthylene	$C_{12}H_8$	152	ACY	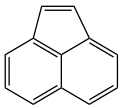
Acenaphthene	$C_{12}H_{10}$	154	ACE	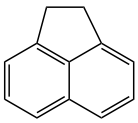
Fluorene	$C_{13}H_{10}$	166	FLU	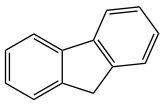
Phenanthrene	$C_{14}H_{10}$	178	PHE	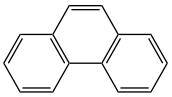
Anthracene	$C_{14}H_{10}$	178	ANT	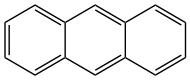
Fluoranthene	$C_{16}H_{10}$	202	PYR	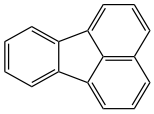
Benzo(a)anthracene	$C_{18}H_{12}$	228	BaA	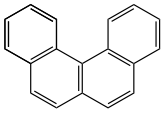
Chrysene	$C_{18}H_{12}$	252	CHRY	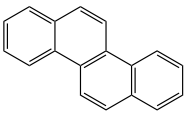
Benzo(a)pyrene	$C_{20}H_{12}$	252	BaP	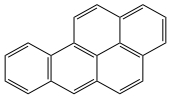
Benzo(b)fluoranthene	$C_{20}H_{12}$	252	BbF	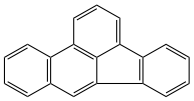
Benzo(k)fluoranthene	$C_{20}H_{12}$	252	BkF	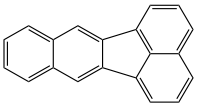
Indeno(1,2,3-d)pyrene	$C_{22}H_{12}$	276	PYR	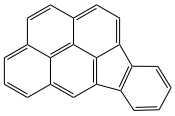
Benzo(g,h,i)perylene	$C_{22}H_{12}$	276	BgP	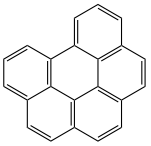
Dibenzo(a,h)anthracen	$C_{22}H_{14}$	278	DhA	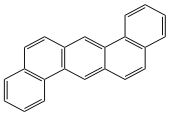

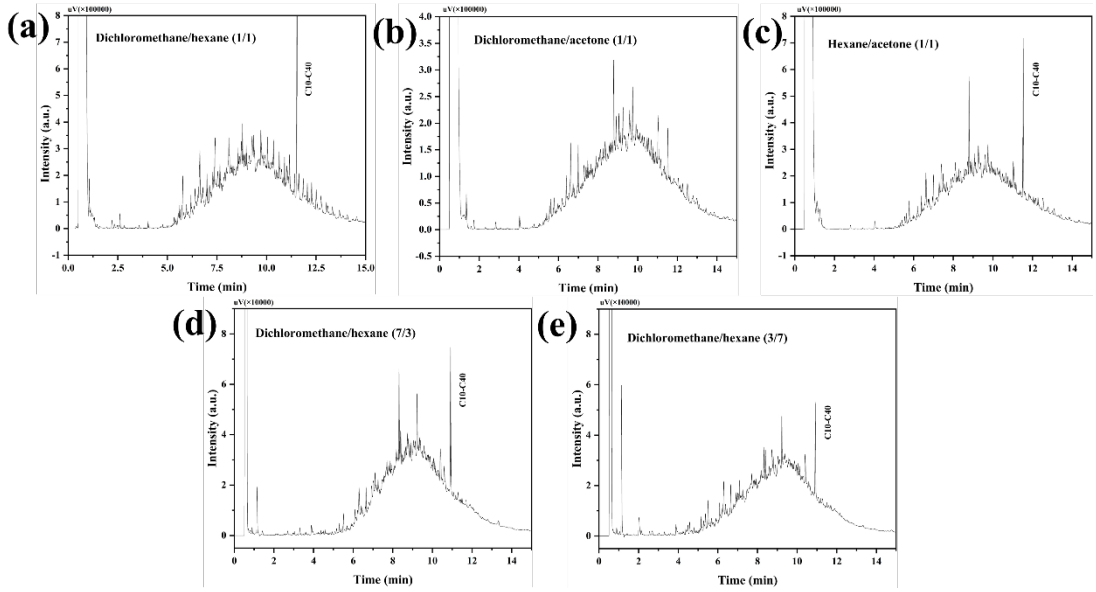

Figure S3. Optimized chromatograms of petroleum hydrocarbon extractants (**a**) dichloromethane/n-hexane (1/1), (**b**) dichloromethane/acetone (1/1), (**c**) n-hexane/acetone (1/1), (**d**) dichloromethane/n-hexane (7/3), (**e**) dichloromethane/n-hexane (3/7).

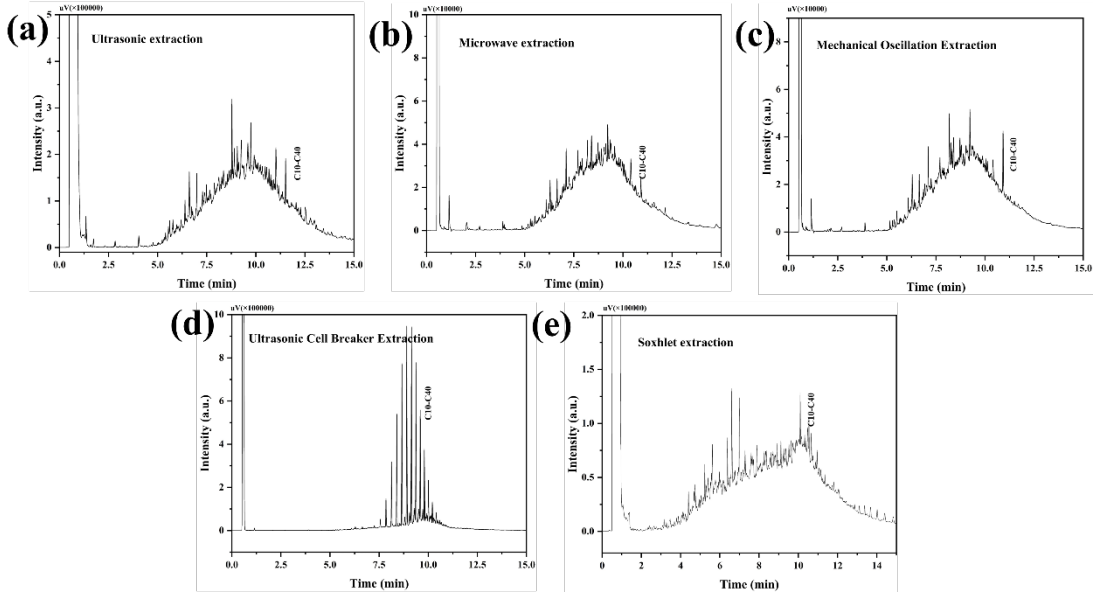

Figure S4. Optimized chromatograms of petroleum hydrocarbon extraction methods (**a**) ultrasonic extraction, (**b**) microwave extraction, (**c**) mechanical oscillation extraction, (**d**) ultrasonic cell breaker extraction, and (**e**) soxhlet extraction.

3.1. Determination of TCE Concentration

For traditional ultrasound extraction, mechanical oscillation extraction, and ultrasonic cell disruptor extraction, n-hexane is commonly employed as the extraction solvent. N-hexane is a non-polar solvent with a low dielectric constant, which does not absorb microwaves and has a minimal heating effect, making it suitable for conventional extraction methods. In microwave-assisted extraction, a mixture of acetone and n-hexane in a 1:1 ratio is selected to leverage the temperature-increasing characteristics of acetone under microwave irradiation, thereby enhancing the efficiency and speed of microwave-assisted extraction. This solvent mixture can accommodate the extraction requirements of both non-polar and polar solutes concurrently, rendering microwave-assisted extraction more effective. The absorbance was detected by UV spectrophotometer at 205 nm, and the standard curve is shown in Figure S5.

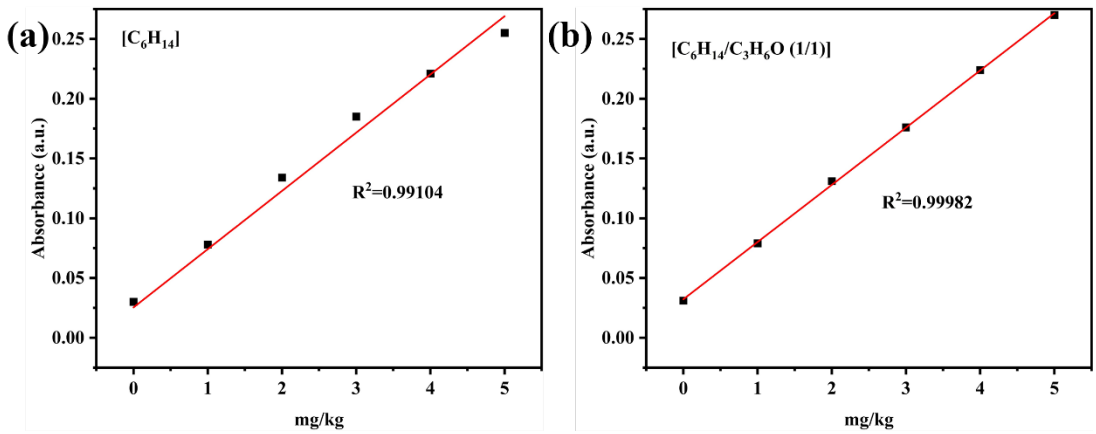

Figure S5. Standard curve (**a**) The extractant was n-hexane, (**b**) The extractant was n-hexane/acetone (1/1).

3.2. RSM Model Fitting

The ultrasonic extraction, microwave extraction, and mechanical oscillation extraction of trichloroethylene were optimized using the Box-Behnken design (BBD) method. The BBD methodology was employed to investigate the impacts of various factors on the extraction process, including liquid-to-solid ratio (1–3 g/mL), extraction time (10–20 min), number of extractions (1–3 times), and extraction temperature (30–60°C). The experimental design and extraction rate of three methods for extraction of trichloroethane-contaminated soil are shown in Table S10–S12. Analysis of Variance (ANOVA) was carried out to evaluate the influence of the independent variables and the significance of the interactions.

Table S10. Experimental design of trichloroethane contaminated soil using ultrasonic extraction and extraction rates.

Run	Liquid-to-Solid Ratio (mL/g)	Extraction Time (min)	Extraction Times	Extraction Temperature (°C)	Extraction Rate (%)
1	2	10	2	30	54.1434
2	2	20	2	30	57.1962
3	2	10	2	60	64.6106
4	3	15	3	45	72.8972
5	1	10	2	45	51.0904
6	2	20	3	45	67.6636
7	2	15	1	30	25.3582
8	1	15	3	45	63.7384
9	2	15	3	30	72.8972
10	2	15	2	45	65.919
11	2	15	2	45	65.919
12	1	20	2	45	50.6542
13	2	10	1	45	0.4984
14	2	20	1	45	17.944
15	2	15	2	45	65.919
16	2	10	3	45	67.6636
17	1	15	2	60	46.729
18	3	10	2	45	40.187
19	3	15	1	45	35.8256
20	2	15	2	45	65.919
21	1	15	1	45	11.4018
22	2	15	2	45	65.919
23	1	15	2	30	40.187
24	3	15	2	30	65.919
25	2	15	1	60	24.0498
26	3	20	2	45	66.3552

27	2	15	3	60	89.4704
28	3	15	2	60	52.3988
29	2	20	2	60	66.7912

Table S11. Experimental design of trichloroethane contaminated soil using mechanical oscillation extraction and extraction rates.

Run	Liquid-to-Solid Ratio (mL/g)	Extraction Time (min)	Extraction Times	Extraction Temperature (°C)	Extraction Rate (%)
1	2	10	2	30	34.081
2	2	20	2	30	43.676
3	2	10	2	60	26.6666
4	3	15	3	45	69.8442
5	1	10	2	45	16.6356
6	2	20	3	45	61.5576
7	2	15	1	30	11.838
8	1	15	3	45	34.9532
9	2	15	3	30	49.3458
10	2	15	2	45	42.3676
11	2	15	2	45	42.3676
12	1	20	2	45	15.7632
13	2	10	1	45	7.9128
14	2	20	1	45	13.1464
15	2	15	2	45	42.3676
16	2	10	3	45	51.0904
17	1	15	2	60	20.1246
18	3	10	2	45	48.4736
19	3	15	1	45	20.9968
20	2	15	2	45	42.3676
21	1	15	1	45	0.4984
22	2	15	2	45	42.3676
23	1	15	2	30	14.4548
24	3	15	2	30	53.271
25	2	15	1	60	17.0716
26	3	20	2	45	58.0686
27	2	15	3	60	61.5576
28	3	15	2	60	44.5482
29	2	20	2	60	38.4424

Table S12. Experimental design of trichloroethane contaminated soil using microwave extraction and extraction rates.

Run	Liquid-to-Solid Ratio (mL/g)	Extraction Time (min)	Extraction Times	Extraction Temperature (°C)	Extraction Rate (%)
1	2.00	10.00	3.00	60.00	51.9626
2	2.00	20.00	2.00	50.00	82.4922
3	3.00	10.00	2.00	60.00	28.4112
4	2.00	15.00	1.00	70.00	14.4548
5	1.00	15.00	3.00	60.00	49.3458
6	3.00	20.00	2.00	60.00	46.729
7	2.00	15.00	2.00	60.00	56.324
8	1.00	10.00	2.00	60.00	20.5608
9	1.00	15.00	1.00	60.00	14.4548
10	1.00	15.00	2.00	50.00	66.7912
11	2.00	15.00	3.00	50.00	89.4704

12	2.00	15.00	3.00	70.00	47.6012
13	2.00	15.00	1.00	50.00	29.7196
14	1.00	15.00	2.00	70.00	35.8256
15	2.00	20.00	3.00	60.00	47.6012
16	2.00	20.00	1.00	60.00	25.3582
17	2.00	15.00	2.00	60.00	56.324
18	2.00	10.00	2.00	70.00	40.187
19	2.00	15.00	2.00	60.00	56.324
20	2.00	10.00	1.00	60.00	22.7414
21	2.00	10.00	2.00	50.00	72.8972
22	2.00	15.00	2.00	60.00	56.324
23	2.00	20.00	2.00	70.00	84.6728
24	2.00	15.00	2.00	60.00	56.324
25	3.00	15.00	2.00	70.00	57.6324
26	3.00	15.00	1.00	60.00	39.3146
27	3.00	15.00	2.00	50.00	84.6728
28	1.00	20.00	2.00	60.00	39.7508
29	3.00	15.00	3.00	60.00	59.377

After variance analysis of the second-order polynomial model (Table S13), regression models with different extraction methods are shown as follows. First, the regression model obtained by ultrasonic extraction showed a high F-value (15.380) and a significant P-value (<0.0001), indicating the significance of the model. The R^2 value is 0.9390, indicating that about 93.90% of the variance of the dependent variable can be explained by the model, and the adjusted coefficient of determination (Adj R^2) is 0.8779, indicating that the model can still fit the data well after adjustment. The coefficient of variation is 13.77%, indicating that the degree of data dispersion is relatively small. The Adeq Precision estimate for the signal-to-noise ratio is 14.780, indicating an appropriate ratio of signal to noise. The regression model obtained by microwave extraction showed a low F-value (5.52) and a significant P-value (0.0015), indicating that the model was statistically significant. The R^2 value is 0.8466, indicating that the model can explain about 84.66% of the variance of the dependent variable, and the adjusted coefficient of determination is 0.6932, indicating that the model can still fit the data more consistently after adjustment. The coefficient of variation is 23.51%, indicating that the data are relatively dispersed. The SNR Adeq Precision of the model is estimated to be 10.004. The regression model obtained by mechanical oscillation method has a high F-value (44.70) and a significant P-value (<0.0001), which verifies the statistical significance of the model. The R^2 value is 0.9781, indicating that about 97.81% of the variance of the dependent variable can be explained by the model, while the adjusted coefficient of determination is 0.9562, indicating that the model can still fit the data very well after adjustment. The coefficient of variation is 10.87%, indicating that the degree of dispersion of the data is relatively small. The SNR Adeq Precision of the model is estimated to be as high as 27.099, which further indicates the adequacy of the polynomial model signa.

Furthermore, in the normal probability plot of the residuals (Figure S6a,d,g), it is observed that the residuals obtained by the three different extraction methods are distributed almost exactly along a straight line, which shows that the difference between the residuals and the normal distribution is small. In this case, we can conclude that the model's residuals fit the normal distribution well. On the other hand, through the distribution of residuals and predicted values Figure S6b,e,h), we can assess whether the model has a heteroscedasticity problem (that is, the variance is not constant). As can be seen from the figure, the data points are evenly distributed in the middle part of the figure, and there is no obvious trend or rule. This shows that the variance of the model is relatively stable in the range of different predicted values and does not change significantly with the change of predicted values. In addition, the distribution of predicted and actual values (as shown in Figure S6c,f,i) is used to evaluate the prediction accuracy of the model. It can be observed from the figure that the predicted and actual values of the three extraction methods are distributed around a roughly 45° diagonal line. This shows that the predicted results of the model are consistent with the actual observed values, and the model can predict the extraction rates of different extraction methods relatively accurately.

In summary, the three extraction methods perform well in statistical modeling, the deviation between residual and normal distribution is small, the variance of the model is relatively stable, and there is consistency between the predicted value and the actual value, which provides support for the reliability and effectiveness of the model.

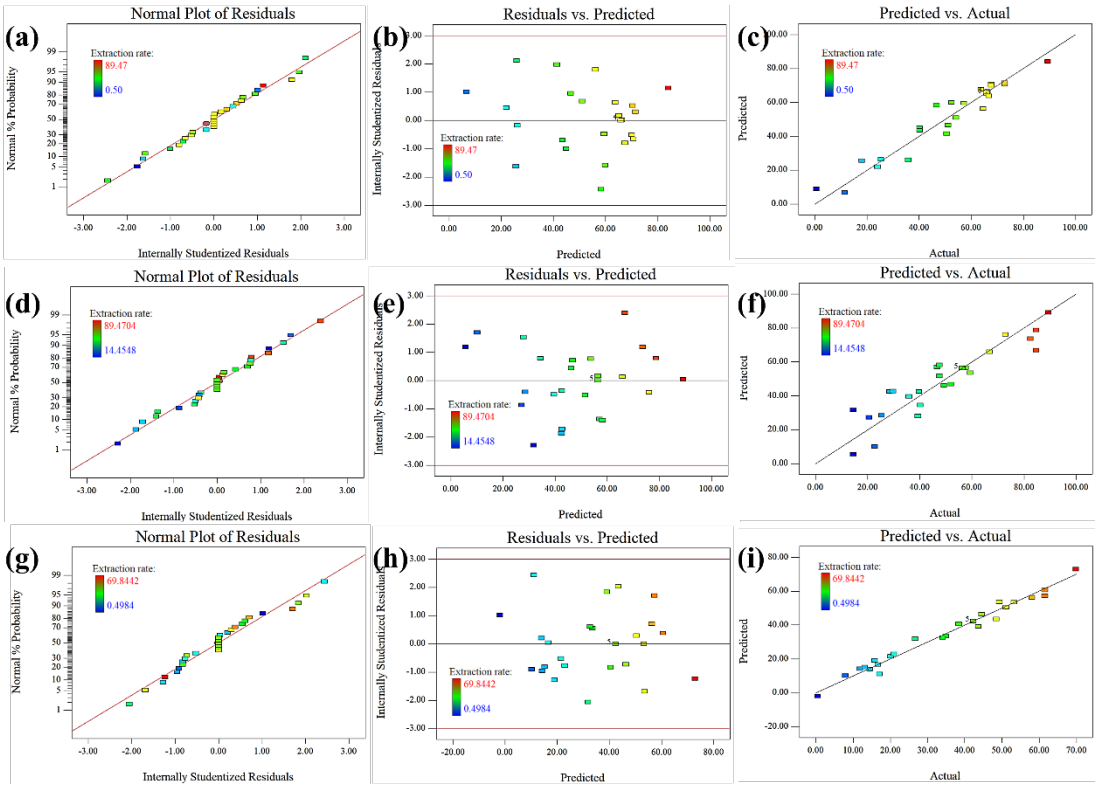

Figure S6. Normal probability distribution of residual, residual and predicted value distribution, predicted and actual value distribution: ultrasonic extraction (**a–c**), microwave extraction (**d–f**), oscillation extraction (**g–i**).

3.3. Effect of Process Variables

By comparing F-values, it can be determined that among the factors affecting the extraction rate, the first-order term C and the quadratic term C^2 reached a highly significant level ($P < 0.01$), while the first-order term A, quadratic term A^2, and B^2 reached a significant level ($P < 0.05$). The effects of the remaining factors were not significant. Considering the significance of the influencing factors, the impact on the extraction rate can be ranked from highest to lowest as follows: extraction frequency > liquid-solid ratio > extraction time > extraction temperature. Notably, extraction frequency is a crucial factor in the ultrasonic extraction process. Regarding the quadratic terms of the factors A, B, C, and D in the equation, it can be observed that they exhibit a negative effect on ultrasonic extraction. This indicates that an increase in the liquid-solid ratio, extraction time, extraction frequency, and extraction temperature to a certain extent leads to a decrease in the extraction rate. Within the ultrasonic extraction regression equation, response surface plots were generated, as depicted in Figure S7a–f. Figure S7a–c illustrate the interaction effects between the liquid-solid ratio and extraction time, extraction frequency, and extraction temperature. From these figures, it is evident that as these variables increase simultaneously, the extraction rate initially rises and then declines. The peak extraction rate is reached when the liquid-solid ratio is 2 mL/g, extraction time is 18 min, extraction temperature is 45 °C, and the extraction frequency is three times. Figure S7d,e portrays the interaction effects between extraction time, extraction frequency, and extraction temperature. In these interactions, the peak extraction rate occurs at an extraction time of 15 min, an extraction frequency of three times, and an extraction temperature of 60 °C. Further insights from Figure S7f lead us to the conclusion that the peak extraction rate approximately appears with an extraction frequency of about three times and an extraction temperature of around 60 °C. Based on the analysis of the response surface plots, an optimized operating scheme was determined: a liquid-solid ratio of 1.77 mL/g, an extraction time of 14.31 min, an extraction frequency of three times, and an extraction temperature of 60 °C. According to this scheme, the predicted extraction rate is 84.49%.

Utilizing the microwave extraction method, the comparative analysis of F-values provides a clear understanding of the impact of different factors on experimental outcomes. In the realm of statistical analysis, we observed that the first-order terms C and D, as well as the quadratic terms A^2 and C^2, exerted a highly significant influence ($P < 0.01$). Simultaneously, the first-order terms A and B, along with the quadratic term

D2, exhibited a significant impact ($P < 0.05$), whereas other factors did not demonstrate significant effects. By evaluating the magnitudes of the respective F-values, we were able to establish a relative hierarchy of factors influencing microwave extraction rate, ranked as follows: extraction frequency > extraction temperature > extraction time > liquid-solid ratio. Furthermore, through response surface plots, we could visually analyze the interplay of dual variables, as depicted in Figure S7g–l. Drawing insights from the analysis of response surface plots, we have identified the optimized operational conditions: a liquid-solid ratio of 2.08 mL/g, an extraction time of 13.93 min, an extraction frequency of three times, and an extraction temperature of 50.03 °C. Under these conditions, the predicted extraction rate stands at 89.51%.

The application of mechanical oscillation-based extraction method allows us to discern the impact of different factors on experimental outcomes through the comparison of F-values. In this context, we found that the first-order terms A, B, and C, as well as the quadratic terms A^2 and C^2, achieved an extremely significant level ($P < 0.01$), while other factors exhibited no significant effects. When comparing the magnitudes of the F-values, we can deduce that the influence of the four factors on extraction rate follows the descending order: liquid-solid ratio > extraction frequency > extraction time > extraction temperature. Furthermore, response surface plots provide a visual analysis of the interaction between dual variables, as illustrated in Figure S7m–r. Drawing insights from the analysis of the response surface plots, we have established an optimized strategy: a liquid-solid ratio of 2.91 mL/g, an extraction time of 15.3 min, an extraction frequency of three times, and an extraction temperature of 35.26 °C. Under these conditions, the predicted extraction rate is 72.20%.

The final multiple regression model equations are as follows:

Extraction rates (Ultrasonic extraction) = $65.92 + 5.82A + 4.03B + 26.60C + 2.36D + 6.65AB - 3.82AC - 5.02AD - 4.36BC - 0.22BD + 4.47CD - 8.52A^2 - 7.60B^2 - 14.52C^2 - 0.73D^2$ (Equation (1))

Extraction Rate (Microwave Extraction) = $56.32 + 7.45A + 7.49B + 16.61C - 12.14D - 0.22AB - 3.71AC + 0.98AD - 1.74BC + 8.72BD - 6.65CD - 8.30A^2 - 5.74B^2 - 14.74C^2 + 12.14D^2$ (Equation (2))

Extraction Rate (Mechanical oscillation extraction) = $42.37 + 16.06A + 3.82B + 21.41C + 0.15D + 2.62AB + 3.60AC - 3.60AD + 1.31BC + 0.55BD + 1.74CD - 5.40A^2 - 3.16B^2 - 5.12C^2 - 3.22D^2$ (Equation (3))

Here, A, B, C, and D represent the liquid-to-solid ratio, extraction time, extraction cycles, and extraction temperature, respectively. AB, AC, AD, BC, BD, and CD denote the interaction terms between the independent variables.

Table S13. ANOVA of quadratic model for ultrasonic extraction, microwave extraction, and mechanical oscillation extraction.

Source	DF	Ultrasonic Extraction				Microwave Extraction				Mechanical Oscillation Extraction			
		SS	MS	F-Value	p-Value	SS	MS	F-Value	p-Value	SS	MS	F-Value	p-Value
Model	14	11,437.270	816.948	15.380	<0.0001*	10434.65	745.33	5.52	0.0015*	9252.225	660.873	44.69602	<0.0001*
A	1	405.794	405.794	7.640	0.0152**	666.15	666.15	4.93	0.0434**	3096.773	3096.773	209.4402	<0.0001*
B	1	195.302	195.302	3.677	0.0758^{ns}	672.66	672.66	4.98	0.0425**	174.759	174.759	11.81926	0.0040*
C	1	8493.519	8493.519	159.904	<0.0001*	3310.53	3310.53	24.51	0.0002*	5499.15	5499.15	371.9172	<0.0001*
D	1	66.971	66.971	1.261	0.280^{ns}	1768.30	1768.30	13.09	0.0028*	0.254	0.254	0.01715	0.8977^{ns}
AB	1	176.949	176.949	3.331	0.0894^{ns}	0.19	0.19	0.00408	0.9706^{ns}	27.392	27.392	1.852543	0.1950^{ns}
AC	1	58.255	58.255	1.097	0.313^{ns}	54.97	54.97	0.41	0.5338^{ns}	51.787	51.787	3.502428	0.0823^{ns}
AD	1	100.623	100.623	1.894	0.190^{ns}	3.85	3.85	0.029	0.8683^{ns}	51.787	51.787	3.502428	0.0823^{ns}
BC	1	76.087	76.087	1.432	0.251^{ns}	12.17	12.17	0.090	0.7684^{ns}	6.848	6.848	0.463118	0.5073^{ns}
BD	1	0.190	0.190	0.00358	0.953^{ns}	304.34	304.34	2.25	0.1555^{ns}	1.189	1.189	0.080412	0.7809^{ns}
CD	1	79.938	79.938	1.505	0.240^{ns}	176.95	176.95	1.31	0.2715^{ns}	12.174	12.174	0.823337	0.3796^{ns}
A^2	1	471.167	471.167	8.870	0.0100**	447.37	447.37	3.31	0.0902^{ns}	188.950	188.950	12.77905	0.0030*
B^2	1	374.268	374.268	7.046	0.0189**	213.90	213.90	1.58	0.2288^{ns}	64.852	64.852	4.386039	0.0549^{ns}
C^2	1	1367.498	1367.498	25.745	0.0002*	1408.89	1408.89	10.43	0.0060*	170.347	170.347	11.52088	0.0044*
D^2	1	3.427	3.427	0.0645	0.803^{ns}	955.84	955.84	7.08	0.0186**	67.110	67.110	4.538751	0.0514^{ns}
Residual	14	743.629	53.116			1890.69	135.05			207.0033	14.78595		
Lack of Fit	10	743.629	74.363			1890.69	189.07			207.0033	20.70033		
Pure Error	4	0	0			0.000	0.000			0	0		
		R^2 = 0.9390	RMSE = 52.94			R^2 = 0.8466	RMSE = 49.44			R^2 = 0.9781	RMSE = 35.37		
		R^2_{adj} = 0.8779	C.V.% = 13.77			R^2_{adj} = 0.6932	C.V.% = 23.51			R^2_{adj} = 0.9562	C.V.% = 10.87		

A: Liquid-solid ratio; B: Extraction time; C: Extraction times; D: Extraction temperature; DF: Degree of Freedom; MS: Mean Square; SS: Sum of Squares; Level of significance: * Significant at $P < 0.01$, ** Significant at $P < 0.05$; ^{ns} Not significant at $P > 0.05$.

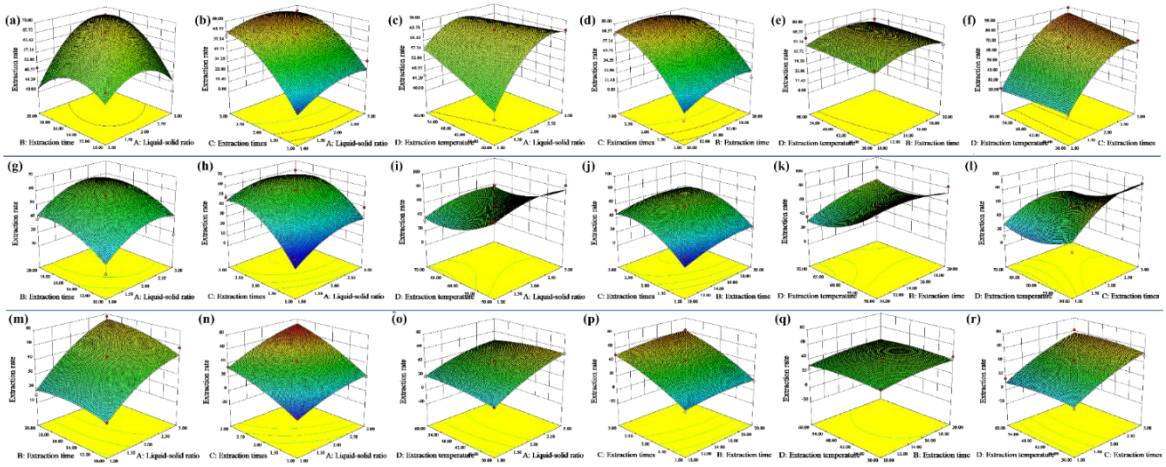

Figure S7. Response surface analysis of ultrasonic extraction (**a**–**f**), microwave extraction (**g**–**l**) and mechanical oscillation extraction (**m**–**r**).

3.4. Ultrasonic Cell Breaker Extraction

Optimization experiments were carried out by varying different parameter settings for the extraction of trichloroethylene from soil using an ultrasonic cell crusher. Based on the results of Figure S8, it can be concluded that the setting of the ultrasonic device with a turn-on time of 1 s followed by a turn-off time of 3 s worked best when the total extraction time was 5 min. It is worth noting that increasing or decreasing the extraction time led to a decrease in extraction efficiency.

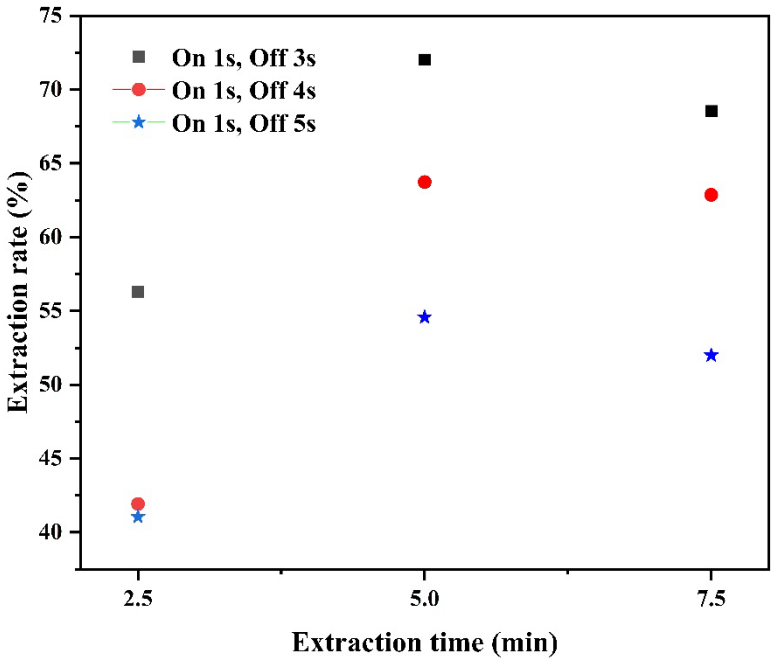

Figure S8. Extraction of TCE by ultrasonic cell crusher at different extraction times (2.5, 5.0, 7.5 min) and different ultrasound on/off times.

4. Biological Stimulus

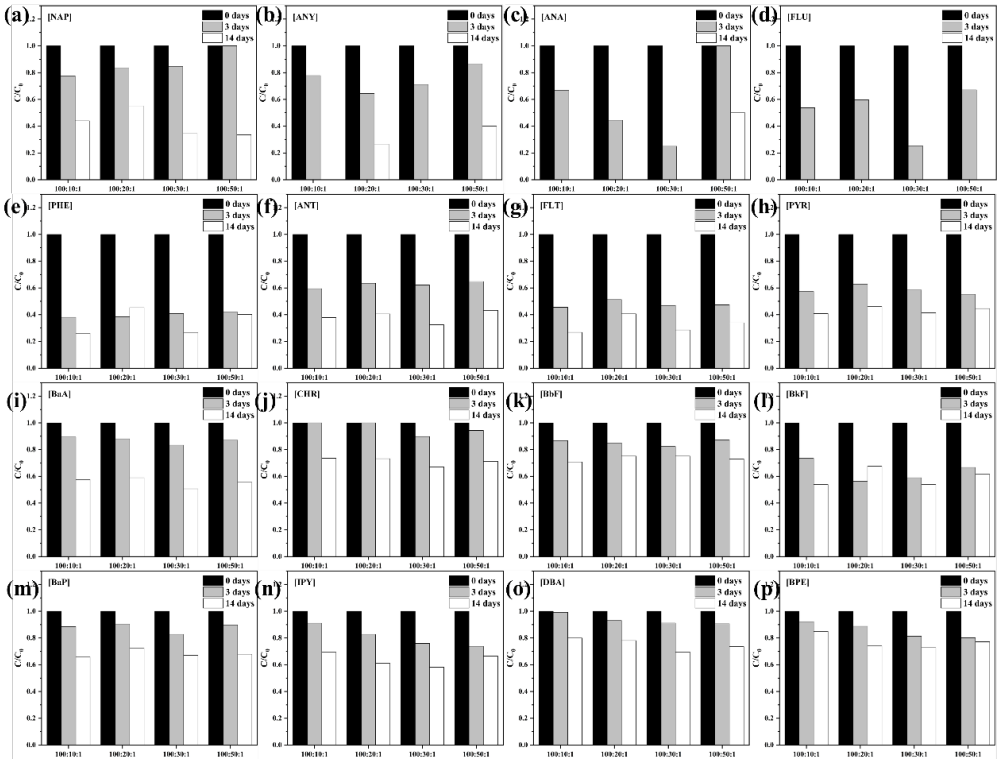

Figure S9. Effect of varying soil carbon/nitrogen/phosphorus ratios (100/10/1, 100/20/1, 100/30/1, 100/50/1) on the degradation of 16 PAHs by natural attenuation, (**a–p**) for NAP, ANY, ANA, FLU, PJE, ANT, FLT, PYR, BaA, CHR, BbF, BkF, BaP, IPY, DBA, BPE.

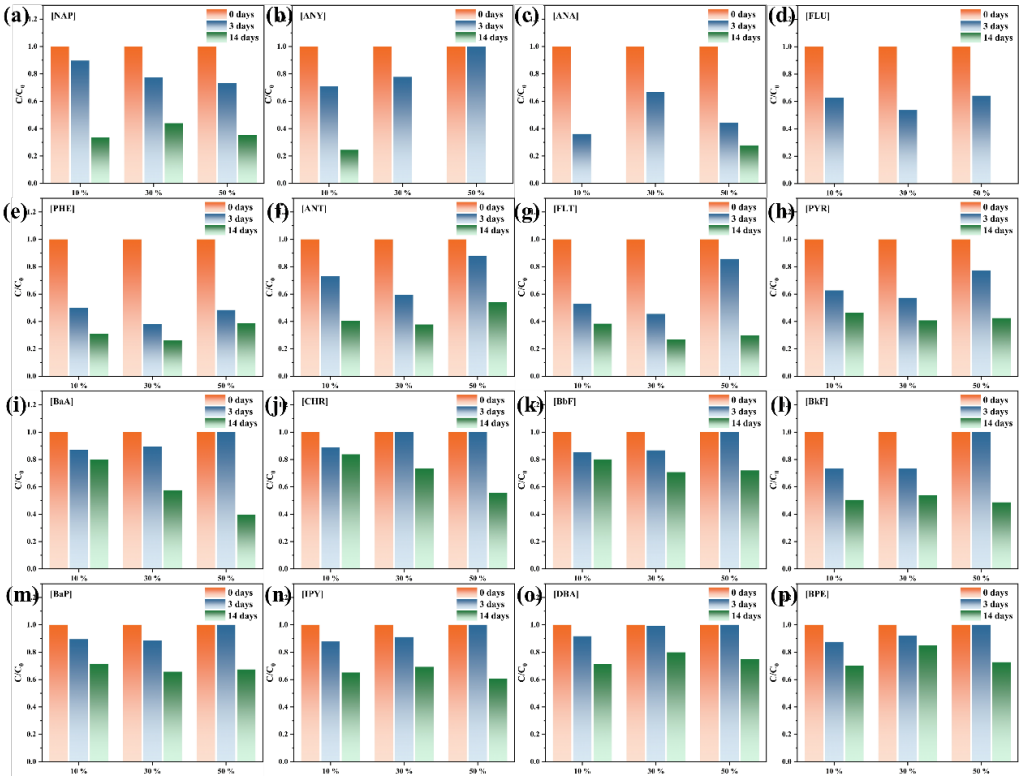

Figure S10. Effect of varying soil moisture content (10%, 30%, 50%) on the natural attenuation degradation of 16 PAHs, (**a–p**) for NAP, ANY, ANA, FLU, PJE, ANT, FLT, PYR, BaA, CHR, BbF, BkF, BaP, IPY, DBA, BPE.

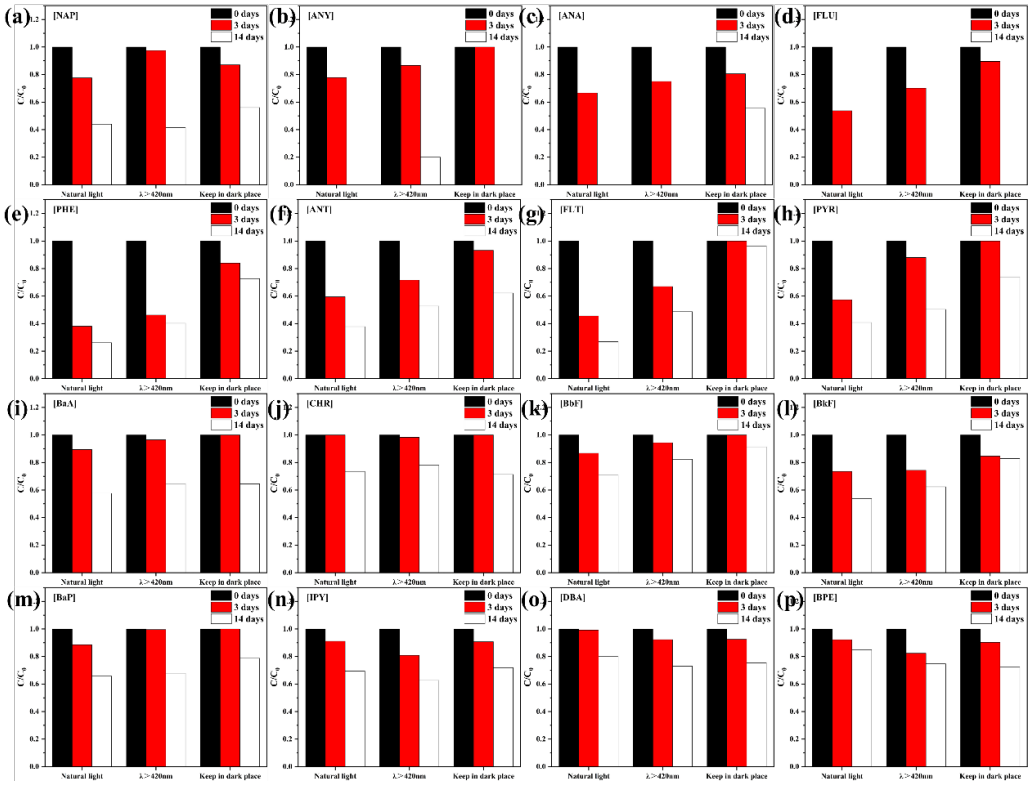

Figure S11. Effect of varying light conditions (natural light, >420 nm, light-avoidance treatment) on the degradation of 16 PAHs by natural attenuation, (**a–p**) for NAP, ANY, ANA, FLU, PJE, ANT, FLT, PYR, BaA, CHR, BbF, BkF, BaP, IPY, DBA, BPE.

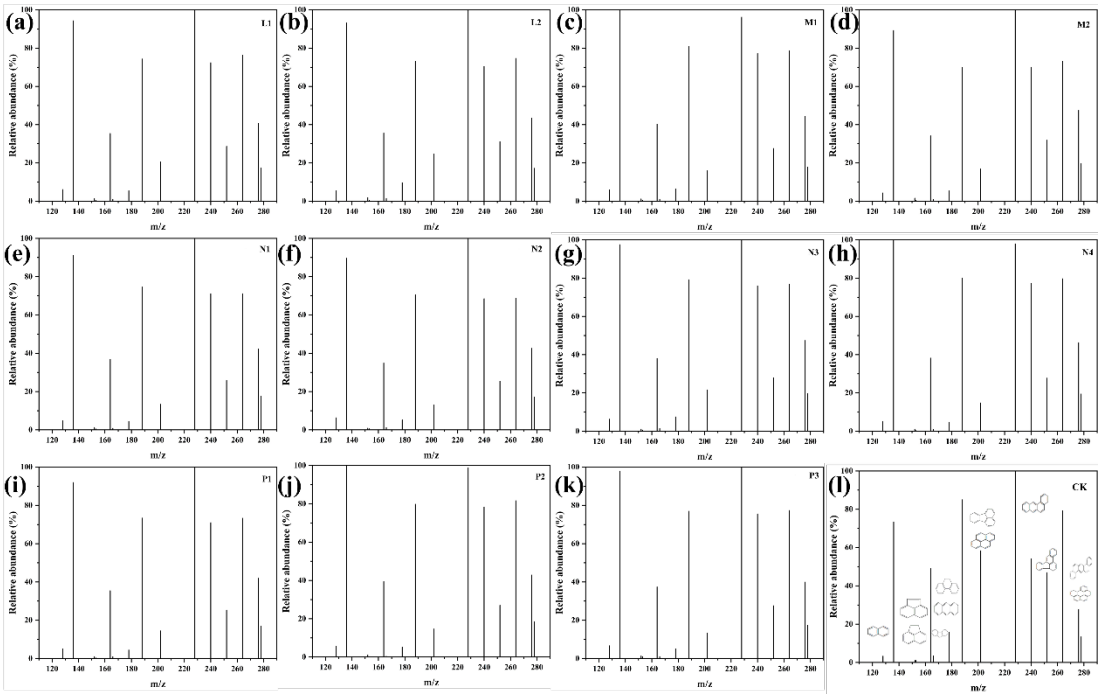

Figure S12. PAHs natural attenuation remediation for 3 days, plots (**a–l**) in order L1, L2, M1, M2, N1, N2, N3, N4, P1, P2, P3, CK (logarithmic scale).

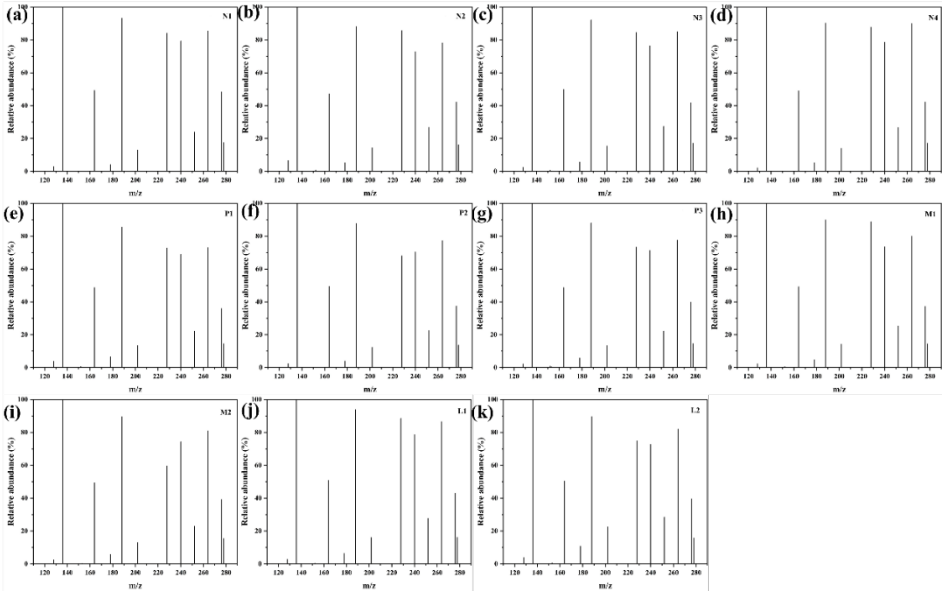

Figure S13. PAHs natural attenuation restoration for 14 days, plots (**a–l**) in order N1, N2, N3, N4, P1, P2, P3, M1, M2, L1, L2.

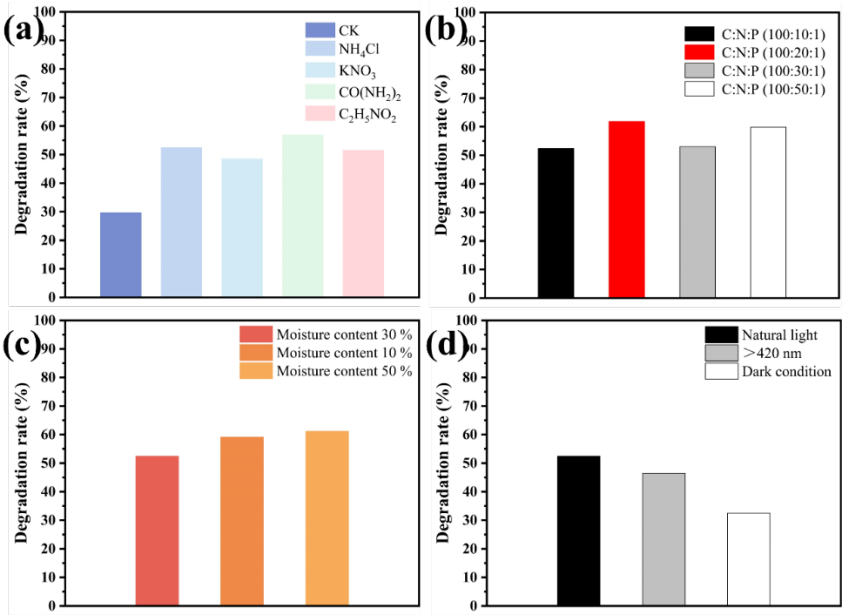

Figure S14. TPHs natural attenuation restoration for 14 days, (**a**) Addition of different nitrogen sources, (**b**) Changing soil carbon, nitrogen and phosphorus ratios, (**c**) Changing soil moisture content, (**d**) Varying light conditions.

5. Combined Remediation with Bioaugmentation and Biostimulation

Table S14. Sequencing data volume and quality statistics of samples.

Sample	B1	B2	CK
Raw_reads	53520	86757	46055
Raw_reads_Q20(%)	97.46	97.72	97.61
Raw_reads_Q30(%)	93.2	93.69	93.72
Merge	51784	84794	44792
Merge (%)	96.76	97.74	97.26
Cutadapt	51149	83837	44269
Cutadapt (%)	95.57	96.63	96.12
Clean_reads	44491	74243	39290

Clean_reads (%)	83.13	85.58	85.31
Clean_reads_Q20 (%)	99.33	99.37	99.41
Clean_reads_Q30 (%)	96.79	96.97	97.12

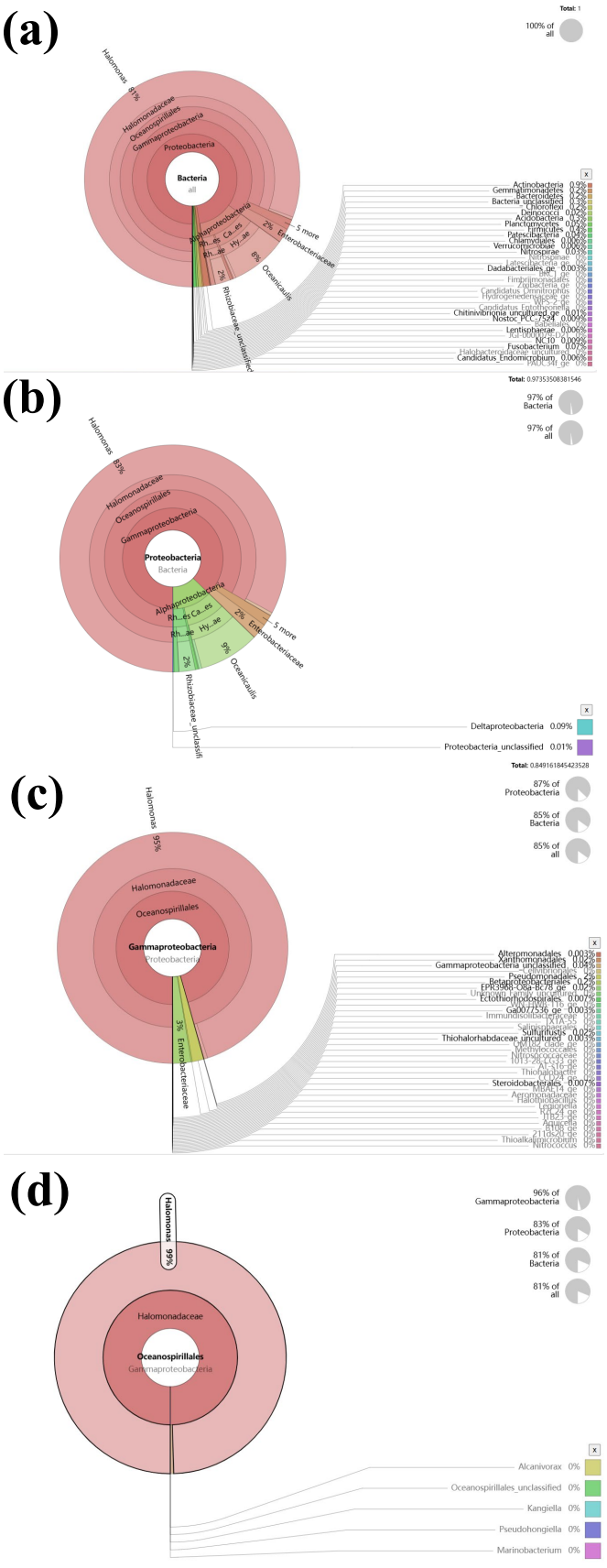

Figure S15. Multilevel species composition of the control group (CK).

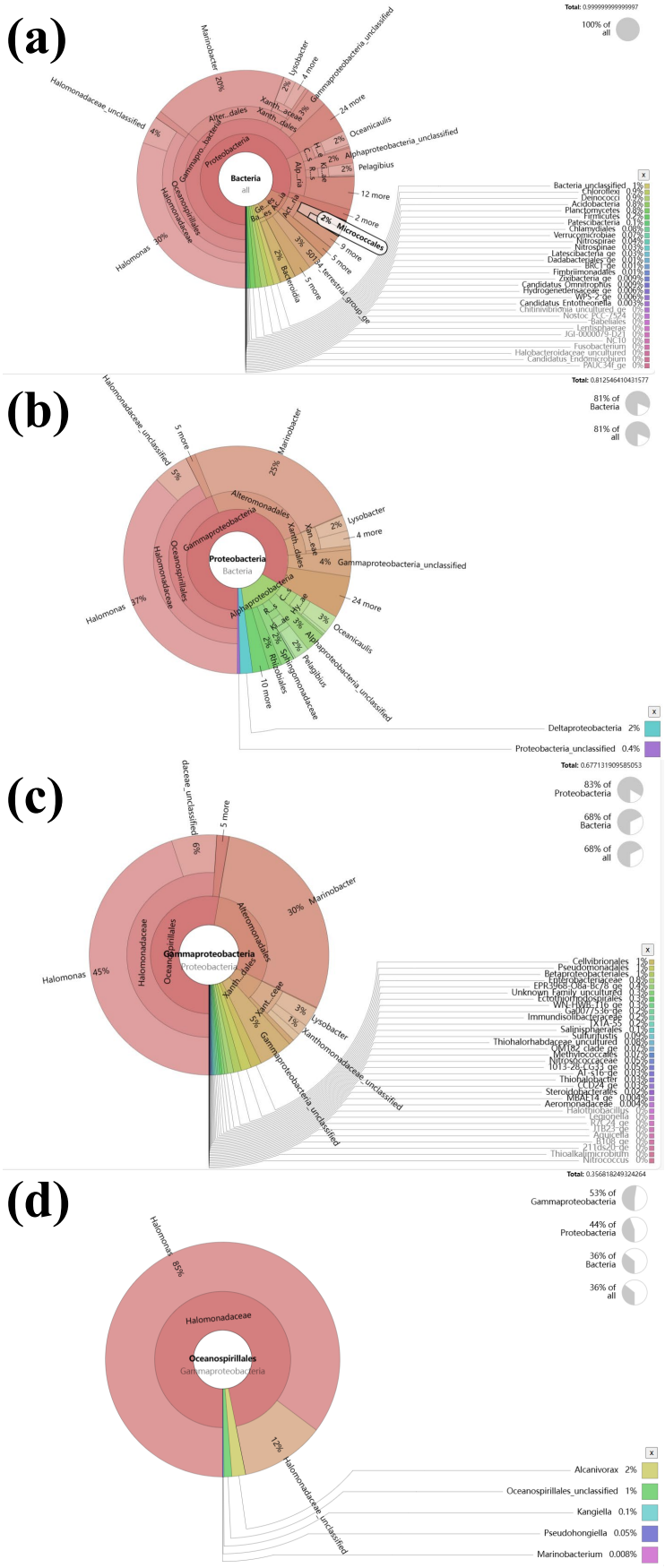

Figure S16. Multilevel species composition of the control group (B1).

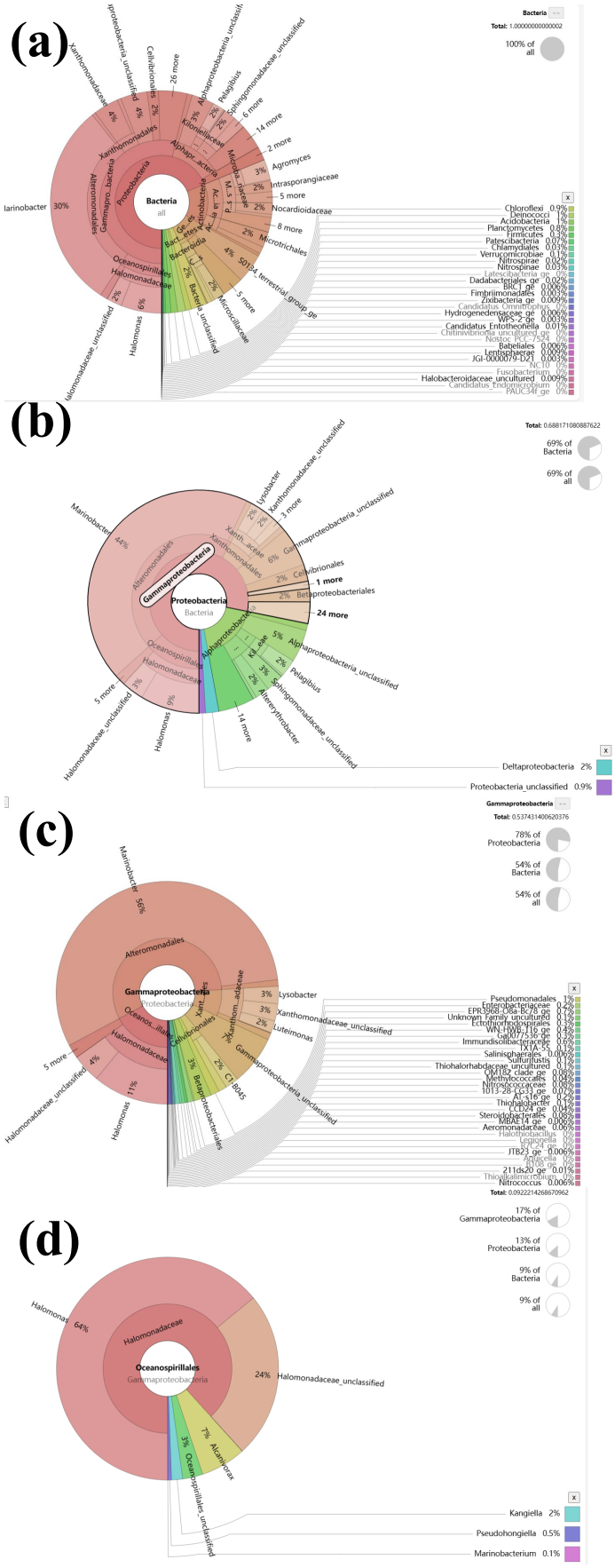

Figure S17. Multilevel species composition of the control group (B2).

Table S15. KEGG_pathway detailed data (level3).

Level 2	B1	B2	CK
Amino acid metabolism	294,695.95	283,851.42	314,157.01
Biosynthesis of other secondary metabolites	40,353.13	38,530.70	44,559.61
Carbohydrate metabolism	292,715.99	281,283.69	320,141.12
Cell growth and death	27,763.91	26,881.39	29,130.48
Cell motility	95,760.30	79,027.71	125,648.08
Cellular community-prokaryotes	7747.92	8532.45	5605.47
Digestive system	155.56	174.96	131.36
Endocrine system	1116.83	1684.97	123.94
Energy metabolism	115,407.45	111,689.69	122,238.88
Environmental adaptation	4380.74	4125.83	4739.49
Excretory system	0.19	0.13	0.06
Folding, sorting and degradation	70,205.41	68,018.76	74,571.07
Glycan biosynthesis and metabolism	61,963.28	57,887.08	66,406.05
Immune disease	6.43	7.41	0.15
Infectious disease: bacterial	1838.75	1673.91	2060.88
Infectious disease: parasitic	1095.26	747.62	1810.42
Lipid metabolism	164,080.23	170,859.74	163,267.16
Membrane transport	45,583.76	42,438.58	51,129.82
Metabolism of cofactors and vitamins	281,376.86	260,315.38	313,646.31
Metabolism of other amino acids	171,322.74	167,158.28	164,629.14
Metabolism of terpenoids and polyketides	169,529.68	175,193.38	160,332.08
Neurodegenerative disease	2546.91	2356.88	0.00
Nucleotide metabolism	34,739.58	32,604.57	38,701.62
Replication and repair	107,542.20	103,505.66	115,667.62
Signal transduction	13,839.33	12,023.48	16,515.52
Signaling molecules and interaction	0.35	0.75	0.00
Transcription	15,176.73	15,958.54	13,643.03
Translation	55,039.82	53,624.37	57,075.96
Transport and catabolism	7389.46	6981.83	8300.17
Xenobiotics biodegradation and metabolism	128,804.89	121,887.90	165,491.54

Table S16. KEGG_pathway Specific hierarchical relationships (level 1–3).

Level 1	Level 2	Level 3	B1	B2	CK
Metabolism	Metabolism of other amino acids	Cyanoamino acid metabolism	15,517	15,672	0
Metabolism	Metabolism of terpenoids and polyketides	Geraniol degradation	26,728	31,102	20,087
Environmental Information Processing	Membrane transport	Bacterial secretion system	19,048	21,024	14,838
Metabolism	Lipid metabolism	Arachidonic acid metabolism	0	5836	0
Metabolism	Xenobiotics biodegradation and metabolism	Caprolactam degradation	15,178	17,430	11,694
Metabolism	Lipid metabolism	Fatty acid biosynthesis	35,906	37,011	31,668
Metabolism	Metabolism of terpenoids and polyketides	Limonene and pinene degradation	11,247	13,331	8597
Metabolism	Xenobiotics biodegradation and metabolism	Aminobenzoate degradation	5787	7261	3451

Metabolism	Xenobiotics biodegradation and metabolism	Bisphenol degradation	3466	4636	1562
Metabolism	Amino acid metabolism	Tryptophan metabolism	15,647	16,891	13,833
Metabolism	Metabolism of terpenoids and polyketides	Biosynthesis of ansamycins	37,316	38,122	35,099
Cellular Processes	Cellular community-prokaryotes	Biofilm formation-Vibrio cholerae	7748	8532	5605
Metabolism	Amino acid metabolism	Lysine degradation	13,691	14,777	12,172
Human Diseases	Neurodegenerative disease	Alzheimer disease	2547	2357	0
Genetic Information Processing	Transcription	RNA polymerase	15,176	15,958	13,643
Metabolism	Xenobiotics biodegradation and metabolism	Fluorobenzoate degradation	2780	3291	983
Metabolism	Lipid metabolism	Biosynthesis of unsaturated fatty acids	16,950	17,569	15,377
Metabolism	Lipid metabolism	Linoleic acid metabolism	2157	2730	641
Metabolism	Glycan biosynthesis and metabolism	Other glycan degradation	1495	2246	323
Metabolism	Metabolism of other amino acids	D-Alanine metabolism	24,556	25,478	23,707
Metabolism	Metabolism of terpenoids and polyketides	Biosynthesis of vancomycin group antibiotics	34,299	34,621	33,066
Genetic Information Processing	Replication and repair	Non-homologous end-joining	1120	1787	408
Metabolism	Lipid metabolism	Fatty acid degradation	25,986	27,069	25,792
Organismal Systems	Endocrine system	Insulin signaling pathway	837	1281	87
Metabolism	Carbohydrate metabolism	Galactose metabolism	8222	8722	7685
Metabolism	Metabolism of cofactors and vitamins	One carbon pool by folate	29,497	29,519	28,489
Metabolism	Metabolism of other amino acids	D-Arginine and D-ornithine metabolism	4920	5118	4115

Table S17. GC-MS results for mixed alkane contaminated soil (0 days).

Retention Time (min)	Area (Abs)	Matched Compound Name	Qualitative	Molecular Weight (amu)	CAS Number	Quantification (%)
6.31	10,382,028	Hexadecane	91	226.27	000544-76-3	0.84
11.12	6,079,526	Heptadecane	94	240.28	000629-78-7	0.49
14.34	5,256,444	Heptadecane	93	240.28	000629-78-7	0.42
14.77	10,758,923	Octadecane	90	254.3	000593-45-3	0.87
15.31	2,843,266	Pentadecane, 2,6,10-trimethyl-	90	254.3	003892-00-0	0.23
25.29	4,284,160	Heneicosane	91	296.34	000629-94-7	0.35
28.96	3,930,035	Heneicosane	90	296.34	000629-94-7	0.32
32.07	5,029,030	Heneicosane	93	296.34	000629-94-7	0.41
16.36	13,956,559	Phenol, 2,2′-methylenebis[6-(1,1-dimethylethyl)-4-methyl-	93	340.24	000119-47-1	1.12
14.84	11,493,987	Pentacosane	90	352.41	000629-99-2	0.93
18.32	6,258,742	Hexacosane	90	366.42	000630-01-3	0.5

31.48	1,356,454	Heptacosane, 1-chloro-	90	414.4	062016-79-9	0.11
31.95	3,091,693	Heptacosane, 1-chloro-	93	414.4	062016-79-9	0.25
11.27	21,322,043	Heptacosane	90	380.44	000593-49-7	1.72
18.48	12,355,949	Hentriacontane	90	436.5	000630-04-6	1
18.6	8,328,566	Hentriacontane	90	436.5	000630-04-6	0.67
22.14	11,102,368	Hentriacontane	90	436.5	000630-04-6	0.89
22.28	6,302,680	Hentriacontane	90	436.5	000630-04-6	0.51
25.64	7,272,487	Hentriacontane	90	436.5	000630-04-6	0.59
25.54	4,084,766	Docosane, 11-decyl-	90	450.52	055401-55-3	0.33
25	4,514,059	Tetracosane, 11-decyl-	90	478.55	055429-84-0	0.36
25.16	2,144,800	Tetracosane, 11-decyl-	90	478.55	055429-84-0	0.17
28.83	3,065,163	Tetratetracontane	90	618.7	007098-22-8	0.25

Table S18. Mass spectra of GC-MS tests of mixed alkane contaminated soils (0 days).

Chromatograms at Different Moments	Quantity/%
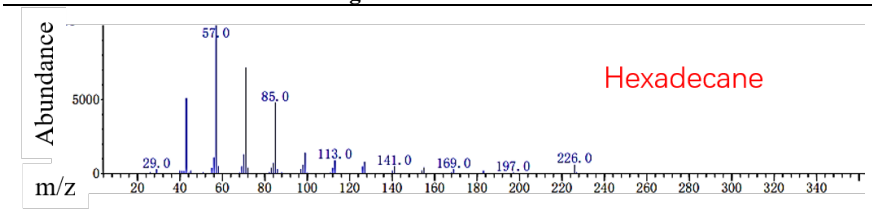	0.84
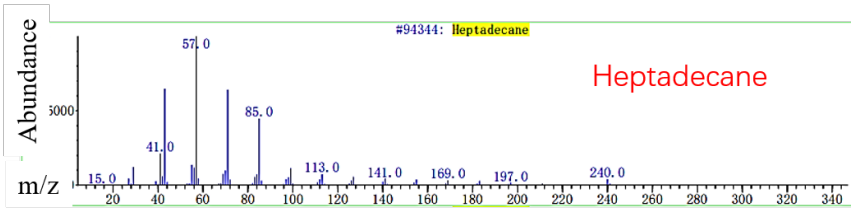	0.91
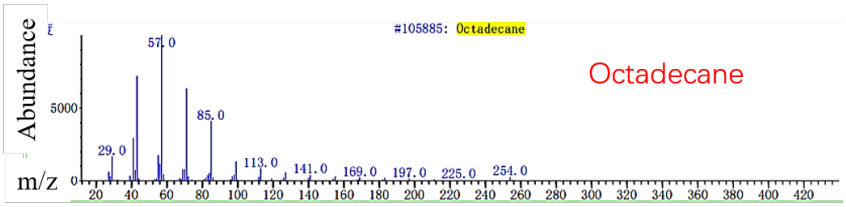	0.87
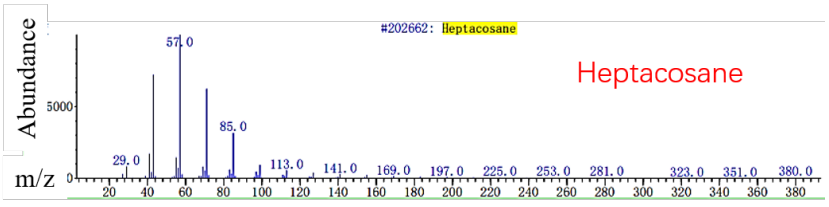	1.72
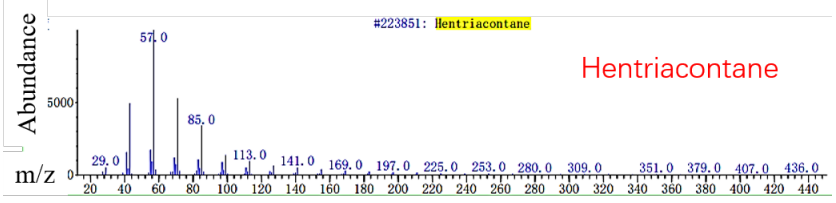	3.66

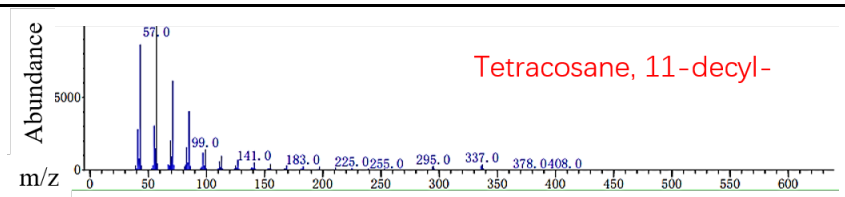	0.53
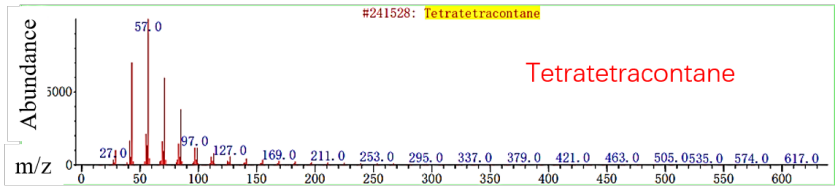	0.25

Table S19. GC-MS results for mixed alkane contaminated soil (30 days).

Retention Time (min)	Area (Abs)	Matched Compound Name	Qualitative	Molecular Weight (amu)	CAS Number	Quantification (%)
5.38	47,609,053	Phenol, 2,4-bis(1,1-dimethylethyl)-	91	206.17	000096-76-4	7.22
8.36	6,760,468	2-Bromotetradecane	90	276.14	074036-95-6	1.03
5.01	48,937,647	Hexadecane	93	226.27	000544-76-3	7.43
6.23	5,797,990	Hexadecane	91	226.27	000544-76-3	0.88
10.79	2,443,093	Heneicosane	90	296.34	000629-94-7	0.37
16.44	8,254,602	Phenol, 2,2′-methylenebis[6-(1,1-dimethylethyl)-4-methyl-	93	340.24	000119-47-1	1.25
7.96	4,750,219	Heptacosane	91	380.44	000593-49-7	0.72
8.07	4,237,799	Octacosane	91	394.45	000630-02-4	0.64
3.25	6,321,474	Methylene chloride	90	83.95	000075-09-2	0.96

Table S20. GC-MS results for mixed alkane contaminated soil (60 days).

Retention Time (min)	Area (Abs)	Matched Compound Name	Qualitative	Molecular Weight (amu)	CAS Number	Quantification (%)
22.84	6,168,180	Octadecane	91	254.3	000593-45-3	0.69
16.41	3,561,140	Phenol,2,2′methylenebis[6-(1,1-dimethylethyl)-4-methyl-	91	340.24	000119-47-1	0.4
11.27	16,949,196	Pentacosane	90	352.41	000629-99-2	1.89
18.49	8,268,456	Pentacosane	91	352.41	000629-99-2	0.92
10.12	5,988,684	Heptadecane, 9-octyl-	90	352.41	007225-64-1	0.67
11.12	5,129,154	Heptadecane, 9-octyl-	90	352.41	007225-64-1	0.57
11.95	6,016,561	Hexacosane	90	366.42	000630-01-3	0.67
14.17	3,487,757	Heneicosane,11-(1-ethylpropyl)-	90	366.42	055282-11-6	0.39
28.83	1,331,903	Heptacosane	90	380.44	000593-49-7	0.15
14.85	6,949,021	Octacosane	90	394.45	000630-02-4	0.78
22.14	7,522,451	Octacosane	91	394.45	000630-02-4	0.84
15.57	2,112,300	2-methyloctacosane	90	408.47	1000376-72-8	0.24
22	4,081,637	2-methyloctacosane	90	408.47	1000376-72-8	0.46
18.6	5,402,641	Hentriacontane	91	436.5	000630-04-6	0.6

25.54	2,723,501	Tetracosane, 11-decyl-	90	478.55	055429-84-0	0.3
14.1	2,084,277	Tetratetracontane	90	618.7	007098-22-8	0.23
3.24	2,326,264	Methylene chloride	91	83.95	000075-09-2	0.26

Table S21. Mass spectra of GC-MS tests of mixed alkane contaminated soils (60 days).

Chromatograms at Different Moments	Quantity/%
	0.15
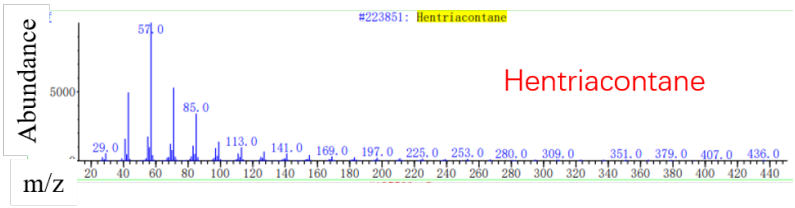	0.60
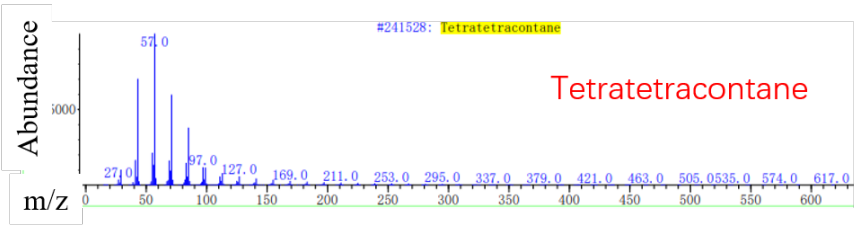	0.23

Table S22. Fukui Index Analysis for tetradecane.

Atom	Number	Charge (0)	Charge (+1)	Charge (−1)	F(0)
C	1	−0.45482	−0.44876	−0.45536	0.0033
C	2	−0.45482	−0.44876	−0.45536	0.0033
C	3	−0.45483	−0.44876	−0.45537	0.0033
C	4	−0.45482	−0.44872	−0.45536	0.0033
C	5	−0.45483	−0.4487	−0.45537	0.0033
C	6	−0.45482	−0.44863	−0.45535	0.0034
C	7	−0.45483	−0.44858	−0.45538	0.0034
C	8	−0.45481	−0.44846	−0.45535	0.0034
C	9	−0.45484	−0.44838	−0.45538	0.0035
C	10	−0.45481	−0.44821	−0.45535	0.0036
C	11	−0.45484	−0.44808	−0.45538	0.0037
C	12	−0.45481	−0.44786	−0.45535	0.0037
C	13	−0.45484	−0.4477	−0.4554	0.0039
C	14	−0.45481	−0.44745	−0.4554	0.0040
C	15	−0.45484	−0.44729	−0.45546	0.0041
C	16	−0.45481	−0.4471	−0.45551	0.0042
C	17	−0.45484	−0.44711	−0.45562	0.0043
C	18	−0.45483	−0.4472	−0.45584	0.0043
C	19	−0.45486	−0.44766	−0.4561	0.0042
C	20	−0.45563	−0.44926	−0.45733	0.0040
C	21	−0.45834	−0.45302	−0.45969	0.0033
C	22	−0.45824	−0.45543	−0.45841	0.0015
C	23	−0.68439	−0.68316	−0.68319	0.0000
C	24	−0.45483	−0.44876	−0.45537	0.0033
C	25	−0.45482	−0.44872	−0.45536	0.0033
C	26	−0.45483	−0.4487	−0.45537	0.0033
C	27	−0.45482	−0.44863	−0.45535	0.0034

C	28	−0.45483	−0.44858	−0.45538	0.0034
C	29	−0.45481	−0.44846	−0.45535	0.0034
C	30	−0.45484	−0.44838	−0.45538	0.0035
C	31	−0.45481	−0.44821	−0.45535	0.0036
C	32	−0.45484	−0.44809	−0.45538	0.0036
C	33	−0.45481	−0.44786	−0.45535	0.0037
C	34	−0.45484	−0.4477	−0.4554	0.0039
C	35	−0.45481	−0.44745	−0.4554	0.0040
C	36	−0.45484	−0.44729	−0.45546	0.0041
C	37	−0.45481	−0.4471	−0.45551	0.0042
C	38	−0.45484	−0.44711	−0.45562	0.0043
C	39	−0.45483	−0.4472	−0.45584	0.0043
C	40	−0.45486	−0.44766	−0.4561	0.0042
C	41	−0.45563	−0.44926	−0.45733	0.0040
C	42	−0.45834	−0.45302	−0.45969	0.0033
C	43	−0.45824	−0.45543	−0.45841	0.0015
C	44	−0.68439	−0.68316	−0.68319	0.0000
H	45	0.22741	0.2355	0.21808	0.0087
H	46	0.22741	0.2355	0.21808	0.0087
H	47	0.22741	0.2355	0.21808	0.0087
H	48	0.22741	0.2355	0.21808	0.0087
H	49	0.22741	0.23551	0.21808	0.0087
H	50	0.22741	0.23551	0.21808	0.0087
H	51	0.22741	0.23554	0.21807	0.0087
H	52	0.22741	0.23554	0.21807	0.0087
H	53	0.22741	0.23558	0.21804	0.0088
H	54	0.22741	0.23558	0.21804	0.0088
H	55	0.22742	0.23565	0.21803	0.0088
H	56	0.22742	0.23565	0.21803	0.0088
H	57	0.22741	0.23571	0.21798	0.0089
H	58	0.22741	0.23571	0.21798	0.0089
H	59	0.22742	0.23582	0.21796	0.0089
H	60	0.22742	0.23582	0.21796	0.0089
H	61	0.22741	0.23591	0.2179	0.0090
H	62	0.22741	0.23591	0.2179	0.0090
H	63	0.22742	0.23604	0.21785	0.0091
H	64	0.22742	0.23604	0.21785	0.0091
H	65	0.22741	0.23615	0.21775	0.0092
H	66	0.22741	0.23615	0.21775	0.0092
H	67	0.22742	0.2363	0.21764	0.0093
H	68	0.22742	0.2363	0.21764	0.0093
H	69	0.22741	0.2364	0.21745	0.0095
H	70	0.22741	0.2364	0.21745	0.0095
H	71	0.22742	0.2365	0.21721	0.0096
H	72	0.22742	0.2365	0.21721	0.0096
H	73	0.22741	0.23651	0.2169	0.0098
H	74	0.22741	0.23651	0.2169	0.0098
H	75	0.22742	0.23647	0.21652	0.0100
H	76	0.22742	0.23647	0.21652	0.0100
H	77	0.22742	0.23626	0.21606	0.0101
H	78	0.22742	0.23626	0.21606	0.0101
H	79	0.22743	0.23591	0.2153	0.0103
H	80	0.22743	0.23591	0.2153	0.0103
H	81	0.22745	0.23534	0.21423	0.0106
H	82	0.22745	0.23533	0.21423	0.0106
H	83	0.22739	0.23445	0.21262	0.0109
H	84	0.22739	0.23445	0.21262	0.0109
H	85	0.227	0.23311	0.21116	0.0110
H	86	0.227	0.23311	0.21116	0.0110

H	87	0.22892	0.23395	0.21514	0.0094
H	88	0.22892	0.23395	0.21514	0.0094
H	89	0.23476	0.24485	0.22203	0.0114
H	90	0.22756	0.23172	0.21747	0.0071
H	91	0.22756	0.23172	0.21747	0.0071
H	92	0.22741	0.23551	0.21808	0.0087
H	93	0.22741	0.23551	0.21808	0.0087
H	94	0.22741	0.23554	0.21807	0.0087
H	95	0.22741	0.23554	0.21807	0.0087
H	96	0.22741	0.23558	0.21804	0.0088
H	97	0.22741	0.23558	0.21804	0.0088
H	98	0.22742	0.23565	0.21803	0.0088
H	99	0.22742	0.23565	0.21803	0.0088
H	100	0.22741	0.23571	0.21798	0.0089
H	101	0.22741	0.23571	0.21798	0.0089
H	102	0.22742	0.23582	0.21796	0.0089
H	103	0.22742	0.23582	0.21796	0.0089
H	104	0.22741	0.23591	0.2179	0.0090
H	105	0.22741	0.23591	0.2179	0.0090
H	106	0.22742	0.23604	0.21785	0.0091
H	107	0.22742	0.23604	0.21785	0.0091
H	108	0.22741	0.23615	0.21775	0.0092
H	109	0.22741	0.23615	0.21775	0.0092
H	110	0.22742	0.2363	0.21764	0.0093
H	111	0.22742	0.2363	0.21764	0.0093
H	112	0.22741	0.2364	0.21745	0.0095
H	113	0.22741	0.2364	0.21745	0.0095
H	114	0.22742	0.2365	0.21721	0.0096
H	115	0.22742	0.2365	0.21721	0.0096
H	116	0.22741	0.23651	0.2169	0.0098
H	117	0.22741	0.23651	0.2169	0.0098
H	118	0.22742	0.23647	0.21652	0.0100
H	119	0.22742	0.23647	0.21652	0.0100
H	120	0.22742	0.23626	0.21606	0.0101
H	121	0.22742	0.23626	0.21606	0.0101
H	122	0.22743	0.23591	0.2153	0.0103
H	123	0.22743	0.23591	0.2153	0.0103
H	124	0.22745	0.23534	0.21423	0.0106
H	125	0.22745	0.23534	0.21423	0.0106
H	126	0.22739	0.23445	0.21262	0.0109
H	127	0.22739	0.23445	0.21262	0.0109
H	128	0.227	0.23311	0.21116	0.0110
H	129	0.227	0.23311	0.21116	0.0110
H	130	0.22892	0.23395	0.21514	0.0094
H	131	0.22892	0.23395	0.21514	0.0094
H	132	0.23476	0.24485	0.22203	0.0114
H	133	0.22756	0.23172	0.21747	0.0071
H	134	0.22756	0.23172	0.21747	0.0071

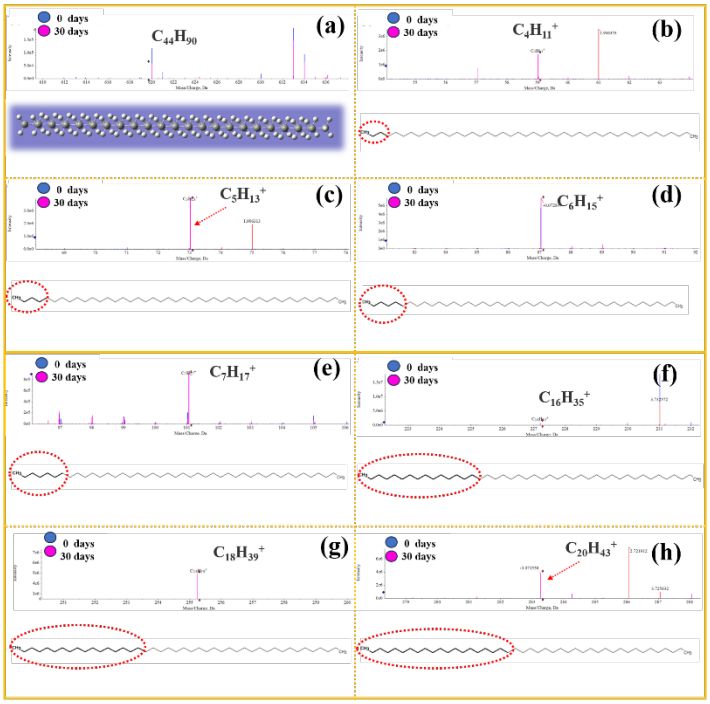

Figure S18. Degradation mechanism of tetradecane in soil.